

# A control mechanism for intramural periarterial drainage via astrocytes: How neuronal activity could improve waste clearance from the brain.

Alexandra K. Diem<sup>a,1</sup>, Roxana O. Carare<sup>b</sup>, Neil W. Bressloff<sup>a</sup>

<sup>a</sup>*Computational Engineering and Design, Faculty of Engineering and the Environment,  
University of Southampton, Southampton, UK*

<sup>b</sup>*Clinical Neurosciences, Faculty of Medicine, University of Southampton, Southampton, UK*

---

## Abstract

The onset and development of Alzheimer's disease (AD) is closely associated with the failure to eliminate waste from the brain [1]. The mechanisms behind this waste clearance remain largely unclear, however research suggests a strong link with the cerebral vasculature [2, 3]. Here we demonstrate computational evidence for a mechanism for cerebral waste clearance that is driven by functional hyperaemia, that is, the dilation of cerebral arteries as a consequence of increased neuronal demand. This mechanism is based on our model for fluid flow through the vascular basement membrane [4]. It accounts for waste clearance rates observed in mouse experiments and aligns with pathological observations as well as recommendations to lower the individual risk of AD, such as keeping mentally and physically active.

**Keywords:** Alzheimer's disease, intramural periarterial drainage, neurovascular unit, neurovascular coupling

---

Alzheimer's disease (AD) is one of the most lethal diseases of the twenty-first century and is closely associated with the failure to eliminate waste products, in particular amyloid- $\beta$  ( $A\beta$ ), from the brain [1]. Experiments on mice have shown that the basement membranes (BM) of the smooth muscle cells (SMC)

---

\*Corresponding author

Email address: A.K.Diem@soton.ac.uk (Alexandra K. Diem)

of cerebral arteries are pathways for the clearance of  $A\beta$ , termed intramural periarterial drainage (IPAD), and have demonstrated that a loss of the pulse results in the failure to clear  $A\beta$  [2, 3], leading to the hypothesis that arterial pulsations due to the heart beat drive IPAD [5, 6, 7, 8]. However, our model demonstrates that arterial pulsations are not strong enough to drive IPAD and thus the exact mechanisms behind waste clearance from the brain remain unclear [4]. Here, using computational simulations, we demonstrate how instead functional hyperaemia, which describes the dilation of cerebral arteries due to an increase in neuronal activity, may provide the driving mechanism. Chemical communication within the neurovascular unit (NVU), which comprises a neuron, an astrocyte and an artery [9], can lead to a dilation of 20 % in a small artery of around 40  $\mu\text{m}$  diameter [10, 11]. Combined with our model of flow through the BM [4] and a finite element (FE) model of an artery wall we demonstrate clearance at a rate comparable to experimental observations [2]. Additionally we demonstrate how this mechanism is impaired by a stiffening of the artery wall, as commonly occurs during age and leads to risk factors for AD such as atherosclerosis [12]. Our mechanism is in line with key pathological features of AD and recommendations to reduce the individual risk of developing AD via physical and mental activity by the Alzheimer’s Society [13].

The brain is the fastest metabolising organ in the body and has unique energy demands. Whilst only taking up 2 % of our body mass it consumes 20 % of our energy [15]. Thus, precise regulation of cerebral blood flow (CBF) is vital in maintaining brain function. Functional hyperaemia is the mechanism by which the NVU increases blood flow to an active region of the brain (Figure 1). The synapses of active neurons release glutamate (Glu) and potassium ( $K^+$ ), which leads to the release of internal  $Ca^{2+}$  stores from the astrocyte via its endfoot into the glia limitans. The SMC membrane is depolarised and the artery dilates [9]. This chemical signalling cascade has been modelled by [11] using ordinary differential equations (ODE), however, a number of equations in the paper contain errors, which are listed and corrected in [14]. The dilation of an artery in response to a stimulus is shown in Figure 2 and the displacement

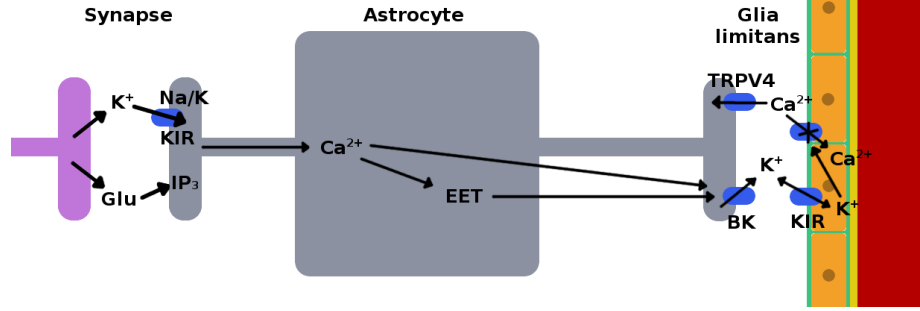


Figure 1: The synapses of active neurons release glutamate (Glu) and potassium ( $K^+$ ).  $K^+$  enters the astrocyte via Na-K pumps and inwardly rectifying  $K^+$  (KIR) channels, whilst Glu receptors in the astrocyte lead to the production of inositol triphosphate ( $IP_3$ ). Internal calcium ( $Ca^{2+}$ ) stores are released and lead to the production of epoxyeicosatrienoic acids (EET), which opens big  $K^+$  (BK) channels at the astrocyte endfoot, releasing  $K^+$ . KIR channels of SMC of the artery activate and increase the extracellular  $K^+$  concentration, which closes  $Ca^{2+}$  channels, decreasing  $Ca^{2+}$  influx into the SMC and dilating the artery. The dilation activates stretch-gated transient receptor potential channels 4 (TRPV4) on the astrocyte endfoot, leading to an influx of extracellular  $Ca^{2+}$  into the astrocyte [9].

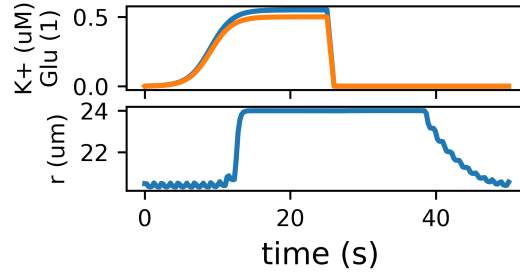


Figure 2: Effect of the release of  $K^+$  and Glu into the synaptic space of a neuron and an astrocyte process. Glu here refers to the ratio of bound/unbound Glu receptors (dimensionless). The arterial radius is modelled using a system of ODE [11] with corrections to the equations listed in [14]. The model shows a dilation of the artery of 20%.

$U(t)$  of the artery is defined as

$$U(t) = r(t) - r_0, \quad (1)$$

where  $r_0$  is the arterial radius at rest.

We modelled an artery wall based on an arteriole with radius  $r_0 = 20 \mu\text{m}$  as a two-dimensional rectangle of height  $h = 4 \mu\text{m}$  and length  $l = 200 \mu\text{m}$  using the FE solver FEniCS [16], using a linear elastic model with the governing equations

$$-\nabla \cdot \sigma = 0 \quad \text{on } \Omega \quad (2)$$

$$\sigma = \lambda(\nabla \cdot u)I + \mu(\nabla u + (\nabla u)^T), \quad (3)$$

where  $\Omega$  describes the domain,  $u$  is the artery wall displacement,  $\sigma$  is the stress tensor,  $I$  is the identity matrix and  $\lambda = 16.44 \text{ MPa}$  and  $\mu = 335.57 \text{ kPa}$  are the Lamé coefficients. The radial boundaries were fixed in space while the longitudinal boundaries were allowed to deform freely. Additionally, an astrocyte was placed centrally on the outer longitudinal boundary, applying the Dirichlet boundary condition

$$u = U(t) \quad \text{on } \partial\Omega_A, \quad (4)$$

where  $\Omega_A$  refers to a section of the outer longitudinal boundary, which models an astrocyte. The optimal mesh consisted of 33,348 triangular elements. The governing equations were solved for 50 s with a time step of 0.25 s, where at each time step the boundary condition (4) was updated.

The rate of IPAD  $q = (q_1, q_2)$  was calculated using our model based on Darcy's law for porous media under thin-film flow conditions [4] in cylindrical coordinates is governed by

$$q = q_1 \mathbf{e}_z + q_2 \mathbf{e}_r = -K \left( \frac{\partial p}{\partial z} \right) \left( \frac{\partial p}{\partial z} \mathbf{e}_z + \frac{\partial p}{\partial r} \mathbf{e}_r \right) \quad (5)$$

$$\frac{\partial q_1}{\partial z} + \frac{1}{r} \frac{\partial}{\partial r} (r q_2) = 0, \quad (6)$$

where  $\mathbf{e}_z$  and  $\mathbf{e}_r$  describe the unit vectors in the  $z$  and  $r$  direction and  $K(\partial p / \partial z)$  describes the permeability of the BM. Permeability is modelled as a step function

$$K\left(\frac{\partial p}{\partial z}\right) = \frac{k}{\mu} \cdot \begin{cases} K_0 & \text{if } \partial p/\partial z < 0, \\ K_1 & \text{otherwise,} \end{cases} \quad (7)$$

where  $k = 1 \times 10^{-12} \text{ cm}^2$  represents the intrinsic permeability of the extracellular matrix,  $\mu = 1.5 \times 10^{-3} \text{ Pa s}$  represents the viscosity of ISF and the ratio  $0 < K_0/K_1 \leq 1.0$  determines the strength of the valve [4]. Applying thin-film flow conditions and kinematic boundary conditions the model equation

$$\frac{\partial}{\partial t} (\gamma \cdot R_i(z, t) \cdot h(z, t)) = \frac{\partial}{\partial z} \left( R_i(z, t) \cdot h(z, t) \cdot K\left(\frac{\partial p}{\partial z}\right) \frac{\partial p}{\partial z} \right) \quad (8)$$

is derived (see [4] for details). The IPAD model requires the pressure gradient along the artery  $\partial p/\partial z$ , which can be recovered directly from the stresses inside the artery wall, such that

$$p = -\sigma_{rr}, \quad (9)$$

where  $\sigma_{rr}$  describes the principal component of  $\sigma$  in the  $r$ -direction [17].

The results are shown in Fig. 3. Displacement and stress inside the artery wall are shown (Fig. 3a) for a single astrocyte of length  $10 \mu\text{m}$  at  $t = 20 \text{ s}$ , where dilation maximal dilation of the artery has been achieved (see Fig. 2). The stress plot shows high stresses at both ends of the artery, which are due to the wall being fixed to  $u = 0$ . Thus, to avoid an influence of these boundary effects on the results all further results are presented for  $10 \mu\text{m} \leq z \leq 190 \mu\text{m}$ . Experimental results from [2] suggest an expected IPAD velocity of  $8 \mu\text{m s}^{-1}$  for the mouse brain, which is adopted as a benchmark value here. Using  $k = 1 \times 10^{-12} \text{ cm}^2$  and  $K_0/K_1 = 0.5$  and average IPAD velocity of  $-8.22 \mu\text{m s}^{-1}$  is achieved, where the negative sign indicates flow in the reverse direction of the blood flow as desired (Fig. 3b). The average flow rate for the same parameters is  $-4.04 \mu\text{l/min}$  for a single arteriole (Fig. 3c). The total length of capillaries in the brain is 400 miles [18]. Estimating the length of an average capillary as  $100 \mu\text{m}$  the number of capillaries in the brain is 6.5 billion. Thus, it would take approximately 17.77 h to process the full volume of ISF (280 ml).

Permeability  $k$  of the extracellular space in the brain is not known, but it ranges between  $1 \times 10^{-14} \text{ cm}^2$  and  $1 \times 10^{-10} \text{ cm}^2$  for interstitial spaces [19].

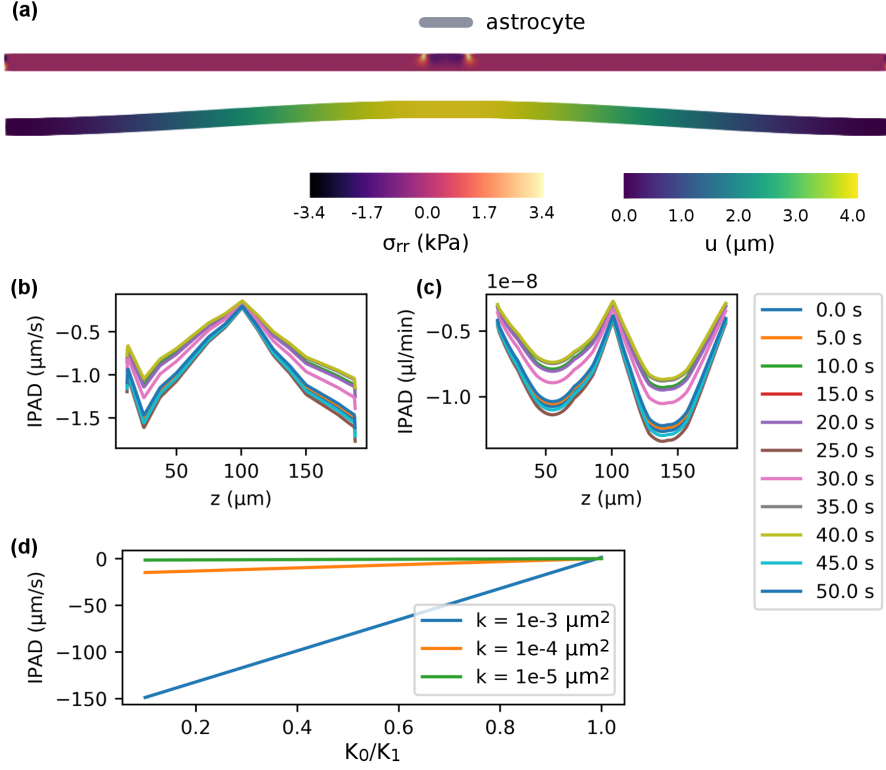


Figure 3: IPAD inside a cerebral artery. (a) Displacement and stress of the artery wall due to  $U(t)$  at  $t = 20\text{ s}$  of a single astrocyte end-foot. Because displacement is fixed to  $u = 0$  at the ends, stresses at the ends are high. Thus, all following results are presented for  $10\text{ }\mu\text{m} \leq z \leq 190\text{ }\mu\text{m}$ . (b) IPAD velocity at various time points over the length of the artery wall using  $K_0/K_1 = 0.5$ . The average velocity over time and space is  $-8.22\text{ }\mu\text{m s}^{-1}$ . (c) IPAD flow rate at various time points over the length of the artery wall using  $K_0/K_1 = 0.5$ . The average flow rate over time and space is  $-4.04 \times 10^{-8}\text{ }\mu\text{l/min}$  for a single arteriole. Extrapolated over 6.5 billion arterioles estimated for the human brain it would take 17.77 h to process the total amount of ISF in the brain (280 ml). (d) IPAD velocity for various values of ECS permeability  $k$  over the strength of the valve mechanisms  $K_0/K_1$ . Values are always negative, except for when  $K_0/K_1 = 1.0$ . The effect of the valve mechanism is decreased with decreasing  $k$ .

Thus it is interesting to observe IPAD velocities for different values of  $k$  and valve strength (Fig. 3d). The target velocity of  $\approx 8 \mu\text{m s}^{-1}$  was achieved for  $k = 1 \times 10^{-12} \mu\text{m s}^{-1}$ , and net velocity is always negative except for  $K_0/K_1 = 1.0$ , i. e. absence of a valve mechanism. A change of the permeability by one order of magnitude results in the same change in the IPAD velocity, thus the effect of the valve mechanism decreases with decreasing  $k$ . Positive net IPAD only occurs for  $K_0/K_1 = 1.0$ , i. e. complete absence of a valve function.

Whilst our model of flow through the BM has previously been used to disprove the well-cited hypothesis that arterial pulsations due to the heart rate drive IPAD [4], combined with a model of neurovascular coupling via astrocytes, it demonstrates a feasible driving mechanism for IPAD. All parameters chosen lie well within physiologically relevant ranges found in the literature. The mechanism produces velocities in accordance with experimental results from [2] and the total estimated flow rate suggests a turnover of ISF just over once a day. Neurovascular coupling is active whenever neurons are active and thus, this theory can explain how both physical and mental activity are considered to reduce one's individual risk.

Our study supports the hypothesis that arterial dilations due to neurovascular coupling may play a crucial role in IPAD. This hypothesis is more intuitive than the previously most cited hypothesis of pulsations due to the heart beat driving IPAD: Athletes have a much lower heart rate than normal, which would put them at increased risk of developing AD under the heart beat hypothesis. However, research shows that regular physical activity acts as one of the best preventive mechanisms [20] and is generally beneficial for cognitive ability [21]. It decreases amyloid load in transgenic mouse models [22] and reduces the risk of hippocampal atrophy in individuals at genetic risk of developing AD [23]. Our neurovascular coupling hypothesis supports and can explain these findings. Physical activity leads to increased neuronal activity, which demands better nutrient supply and, according to our model, is accompanied by increased IPAD and thus decreased amyloid load. Analogously, the same recommendation applies more generally for any cognitively engaging type of activity [24, 25, 26]

and is equally well explained by our hypothesis and supported by our model. In addition our hypothesis supports the findings that cardiovascular diseases such as atherosclerosis and hypertension pose risk factors for AD [12], most likely via two mechanisms: a decreased response to the astrocyte due to a stiffening of the artery wall and stagnating IPAD due to a dysfunction of the valve mechanism. We conclude that our neurovascular hypothesis of the mechanism behind IPAD offers suitable explanations for cardiovascular findings associated with AD and should thus act as the new working hypothesis for the mechanism behind IPAD.

### Acknowledgements

This work was supported by an EPSRC Doctoral Training Partnership grant (EP/N509747/1).

### References

- [1] A. W. J. Morris, R. O. Carare, S. Schreiber, C. A. Hawkes, The cerebrovascular basement membrane: Role in the clearance of  $\beta$ -amyloid and cerebral amyloid angiopathy, *Frontiers in Aging Neuroscience* 6 (2014) 251. doi:10.3389/fnagi.2014.00251.
- [2] R. O. Carare, M. Bernardes-Silva, T. A. Newman, A. M. Page, J. A. R. Nicoll, V. H. Perry, R. O. Weller, Solutes, but not cells, drain from the brain parenchyma along basement membranes of capillaries and arteries: Significance for cerebral amyloid angiopathy and neuroimmunology, *Neuropathology and Applied Neurobiology* 34 (2) (2008) 131–144. doi:10.1111/j.1365-2990.2007.00926.x.
- [3] M. Arbel-Ornath, E. Hudry, K. Eikermann-Haerter, S. Hou, J. L. Gregory, L. Zhao, R. A. Betensky, M. P. Frosch, S. M. Greenberg, B. J. Bacskaï, Interstitial fluid drainage is impaired in ischemic stroke and Alzheimer’s disease mouse models, *Acta Neuropathologica* 126 (3) (2013) 353–364. doi:10.1007/s00401-013-1145-2.



- [4] A. K. Diem, M. MacGregor Sharp, M. Gatherer, N. W. Bressloff, R. O. Carare, G. Richardson, Arterial pulsations cannot drive intramural periarterial drainage: Significance for A $\beta$  drainage, *Frontiers in Neuroscience* 11 (2017) 475. doi:10.3389/fnins.2017.00475.
- [5] R. O. Weller, D. Boche, J. A. R. Nicoll, Microvasculature changes and cerebral amyloid angiopathy in Alzheimer's disease and their potential impact on therapy, *Acta Neuropathologica* 118 (1) (2009) 87–102. doi:10.1007/s00401-009-0498-z.  
URL <http://link.springer.com/10.1007/s00401-009-0498-z>
- [6] J. J. Iliff, M. Wang, Y. Liao, B. A. Plogg, W. Peng, G. A. Gundersen, H. Benveniste, G. E. Vates, R. Deane, S. A. Goldman, E. A. Nagelhus, M. Nedergaard, A Paravascular Pathway Facilitates CSF Flow Through the Brain Parenchyma and the Clearance of Interstitial Solutes, Including Amyloid , *Science Translational Medicine* 4 (147) (2012) 147ra111–147ra111. arXiv:CD004796, doi:10.1126/scitranslmed.3003748.  
URL <http://stm.sciencemag.org/cgi/doi/10.1126/scitranslmed.3003748>
- [7] M. Asgari, D. de Zélécourt, V. Kurtcuoglu, How astrocyte networks may contribute to cerebral metabolite clearance, *Scientific Reports* 5 (2015) 15024. doi:10.1038/srep15024.  
URL <http://www.nature.com/articles/srep15024>
- [8] M. K. Sharp, A. K. Diem, R. O. Weller, R. O. Carare, Peristalsis with Oscillating Flow Resistance: A Mechanism for Periarterial Clearance of Amyloid Beta from the Brain, *Annals of Biomedical Engineering* 44 (5) (2016) 1553–1565. doi:10.1007/s10439-015-1457-6.
- [9] P. G. Haydon, G. Carmignoto, Astrocyte Control of Synaptic Transmission and Neurovascular Coupling, *Physiology Reviews* 86 (2006) 1009–1031. doi:10.1152/physrev.00049.2005.

- [10] H. Farr, T. David, Models of neurovascular coupling via potassium and EET signalling, *Journal of Theoretical Biology* 286 (1) (2011) 13–23. doi:10.1016/j.jtbi.2011.07.006.  
URL <http://dx.doi.org/10.1016/j.jtbi.2011.07.006>
- [11] A. Witthoft, G. E. Karniadakis, A bidirectional model for communication in the neurovascular unit, *Journal of Theoretical Biology* 311 (2012) 80–93. doi:10.1016/j.jtbi.2012.07.014.  
URL <http://dx.doi.org/10.1016/j.jtbi.2012.07.014>
- [12] L. Østergaard, R. Aamand, E. Gutiérrez-Jiménez, Y. C. L. Ho, J. U. Blicher, S. M. Madsen, K. Nagenthiraja, R. B. Dalby, K. R. Drasbek, A. Møller, H. Brændgaard, K. Mouridsen, S. N. Jespersen, M. S. Jensen, M. J. West, The capillary dysfunction hypothesis of Alzheimer’s disease, *Neurobiology of Aging* 34 (4) (2013) 1018–1031. doi:10.1016/j.neurobiolaging.2012.09.011.  
URL <http://dx.doi.org/10.1016/j.neurobiolaging.2012.09.011>
- [13] Alzheimer’s Society, Factsheet: Risk factors for dementia, Tech. Rep. April (2016).  
URL [https://www.alzheimers.org.uk/download/downloads/id/1770/factsheet\\_{\\_}risk\\_{\\_}factors\\_{\\_}for\\_{\\_}dementia.pdf](https://www.alzheimers.org.uk/download/downloads/id/1770/factsheet_{_}risk_{_}factors_{_}for_{_}dementia.pdf)
- [14] A. K. Diem, Chemical Signalling in the Neurovascular Unit, *ReScience* (2017) under review.
- [15] B. V. Zlokovic, The Blood-Brain Barrier in Health and Chronic Neurodegenerative Disorders, *Neuron* 57 (2) (2008) 178–201. doi:10.1016/j.neuron.2008.01.003.
- [16] M. S. Alnaes, J. Blechta, J. Hake, A. Johansson, B. Kehlet, A. Logg, C. Richardson, J. Ring, M. E. Rognes, G. N. Wells, The FEniCS Project Version 1.5, *Archive of Numerical Software* 3. doi:10.11588/ans.2015.100.20553.

- [17] A. K. Diem, Prediction of Perivascular Drainage of Ab from the Brain Using Computational Modelling: Implications for Alzheimer’s Disease, Phd thesis, University of Southampton (2016).
- [18] A. R. Nelson, M. D. Sweeney, A. P. Sagare, B. V. Zlokovic, Neurovascular dysfunction and neurodegeneration in dementia and Alzheimer’s disease, *Biochimica et Biophysica Acta* 1862 (5) (2016) 887–900. [arXiv:15334406](#), [doi:10.1016/j.bbadis.2015.12.016](#).  
URL <http://dx.doi.org/10.1016/j.bbadis.2015.12.016>
- [19] J. R. Levick, Flow through interstitium and other fibrous matrices., *Quarterly journal of experimental physiology* (Cambridge, England) 72 (4) (1987) 409–437. [doi:10.1113/expphysiol.1987.sp003085](#).  
URL <http://www.ncbi.nlm.nih.gov/pubmed/3321140>
- [20] J. L. Woodard, M. A. Sugarman, K. A. Nielson, J. C. Smith, M. Seidenberg, S. Durgerian, A. Butts, N. Hantke, M. Lancaster, M. A. Matthews, S. M. Rao, Lifestyle and genetic contributions to cognitive decline and hippocampal structure and function in healthy aging., *Current Alzheimer Research* 9 (4) (2012) 436–46. [arXiv:NIHMS150003](#), [doi:10.2174/156720512800492477](#).
- [21] F. Gomez-Pinilla, C. H. Hillman, The Influence of Exercise on Cognitive Abilities, *Comprehensive Physiology* 3 (1) (2013) 403–428. [doi:10.1002/cphy.c110063](#).The.
- [22] P. A. Adlard, V. M. Perreau, V. Pop, C. W. Cotman, Voluntary Exercise Decreases Amyloid Load in a Transgenic Model of Alzheimer’s Disease, *Journal of Neuroscience* 25 (17) (2005) 4217–4221. [doi:10.1523/JNEUROSCI.0496-05.2005](#).
- [23] J. C. Smith, K. A. Nielson, J. L. Woodard, M. Seidenberg, S. Durgerian, K. E. Hazlett, C. M. Figueroa, C. C. Kandah, C. D. Kay, M. A. Matthews,

- S. M. Rao, Physical activity reduces hippocampal atrophy in elders at genetic risk for Alzheimer's disease, *Frontiers in Aging Neuroscience* 6 (2014) 61. doi:10.3389/fnagi.2014.00061.
- [24] N. Scarmeas, G. Levy, M.-X. Tang, J. Manly, Y. Stern, Influence of leisure activities on the incidence of Alzheimer's Disease, *Neurology* 57 (12) (2001) 2236–2242. arXiv:NIHMS150003, doi:10.1002/ana.22528.Toll-like.
- [25] R. S. Wilson, D. A. Bennett, J. L. Bienias, N. T. Aggarwal, C. F. Mendes De Leon, M. C. Morris, J. a. Schneider, D. a. Evans, Cognitive activity and incident AD in a population-based sample of older persons., *Neurology* 59 (12) (2002) 1910–1914. doi:10.1212/01.WNL.0000036905.59156.A1.
- [26] L. Fratiglioni, S. Paillard-Borg, B. Winblad, An active and socially integrated lifestyle in late life might protect against dementia, *Lancet Neurology* 3 (6) (2004) 343–353. doi:10.1016/S1474-4422(04)00767-7.